Rigidity-Controlled Crossover: From Spinodal to Critical Failure

Hudson Borja da Rocha[1,2,*] and Lev Truskinovsky[2,†]
[1]LMS, CNRS-UMR 7649, Ecole Polytechnique, Université Paris-Saclay, 91128 Palaiseau, France
[2]PMMH, CNRS-UMR 7636 PSL-ESPCI, 10 Rue Vauquelin, 75005 Paris, France

(Received 23 July 2019; revised manuscript received 15 October 2019; published 8 January 2020)

Failure in disordered solids is accompanied by intermittent fluctuations extending over a broad range of scales. The implied scaling has been previously associated with either spinodal or critical points. We use an analytically transparent mean-field model to show that both analogies are relevant near the brittle-to-ductile transition. Our study indicates that in addition to the strength of quenched disorder, an appropriately chosen global measure of rigidity (connectivity) can be also used to tune the system to criticality. By interpreting rigidity as a timelike variable we reveal an intriguing parallel between earthquake-type critical failure and Burgers turbulence.

DOI: 10.1103/PhysRevLett.124.015501

Failure in disordered solids takes place when elasticity (reversibility) breaks down [1]. The implied abrupt mechanical degradation can be associated with brittle rupture [2], large plastic avalanche [3], or result from other nucleation type macroscopic event [4]. In strain controlled experiments, failure may be accompanied by a dramatic stress drop, and the challenge is to predict and control such undesirable events.

The mechanism of failure in random elastic systems is nontrivial because of the intricate interplay between threshold-type nonlinearity, quenched disorder and long-range interactions. While the strength of disorder, the system size, and the range of elastic interactions are known to affect the failure mechanism [5–8], here we focus on the role of system's *rigidity*, which has recently emerged as another relevant factor in failure-related phenomena [9–11].

Failure in disordered solids is characterized by scale-free statistics of large events. The associated intermittency has been linked to the existence of either spinodal [3,12–15] or critical points [7,16–18]. At large disorder and infinite system size, failure is known to be linked to percolation [19–23]; however, the physical nature of failure at finite disorder remains a subject of debate [3,7,18,24].

In this Letter, we use an analytically tractable mean-field model to show that both spinodal and critical scaling behaviors can coexist near the threshold of the brittle-to-ductile transition [25–31]. Ductile response is understood here in the sense of stable development of small avalanches representing microfailure events [32,33]. Brittle response necessarily involves large events representing system size instabilities [34,35].

Our starting point is the fiber bundle model (FBM) with global stress redistribution [36]. This model was used to explain a variety of physical phenomena from failure of textiles [37], and acoustic emission in loaded composites [38] to earthquake dynamics [39]. It is usually studied in the *stress* control setting, where failure is brittle and scaling is spinodal [2,40]. To address failure under *strain* control and to be able to tune the system to criticality, we drive the system differently, using an external harmonic spring [4,41].

In our analysis, brittle failure emerges as a supercritical, while ductile failure as a subcritical phenomenon. The critical behavior can be associated with the brittle-to-ductile transition and we show that due to superuniversality of mean-field models [42], the equilibrium and out-of-equilibrium exponents are the same.

The main focus of this Letter, however, is the role of system's rigidity [43] as the regulator of the brittle-to-ductile transition. It is known that rigid, crystal-like solids subjected to stresses fail catastrophically [44]. Instead loose, marginally jammed solids fail gradually [9–11]. In view of the minimal nature of our model we could construct analytically the rigidity-disorder phase diagram delineating the domain of ductile behavior at low rigidity and high disorder, from the domain of brittle behavior at low disorder and high rigidity.

One of our crucial findings is that in the brittle-to-ductile crossover region, which bridges *robust* spinodal criticality with *tuned* classical criticality, the transitional exponents are nonuniversal, depending sensitively on system size, disorder, and rigidity. We also show that when rigidity can be conditioned by the system size, failure becomes brittle in the thermodynamic limit, and scaling survives only as a finite size effect, cf. [7,9].

Equilibrium (static) avalanches, corresponding to jumps between different globally minimizing configurations, have been previously linked to Burgers shocks [45,46]. Here we extend this analogy showing that if rigidity is interpreted as "time," and strain as "space," the brittle-to-ductile transition and the associated critical behavior can be viewed as a "finite time" Burgers turbulence [47]. Given

that our model is essentially a mean-field version of the Burridge-Knopoff model [39], the developed analogy reinforces a conceptual link between earthquakes (fracture) and turbulence [48].

Consider a discrete system with dimensionless energy:

$$\mathcal{H} = \frac{1}{N}\sum_{i=1}^{N}\left[u_i(x_i) + \frac{\lambda}{2}(X - x_i)^2\right] + \frac{\Lambda}{2}(\varepsilon - X)^2, \quad (1)$$

where $u_i(x)$ is a Lennard-Jones type potential of a breakable element, X is a Weiss-type mean field accounting for the interaction among breakable elements, and ε is the controlling parameter representing the harmonic interaction of the field X with the loading device, see Fig. 1(a). For determinacy, we assume that the potential $u_i(x)$ is piecewise quadratic: $u_i(x) = (x^2/2)\Theta(l_i - x) + (l_i^2/2)\Theta(x - l_i)$, where Θ is the Heaviside function; for $x \le l_i$, the element is intact, while for $x > l_i$, it is broken. Here, l_i are random numbers drawn from the probability distribution $f(l)$. In our numerical illustrations, we use Weibull's distribution with density $f(x) = \rho x^{\rho-1}\exp(-x^{\rho})$; broad disorder corresponds to small ρ [49]. In our generalization of the FBM (1), we introduced two new parameters: the internal stiffness λ, and the external stiffness $\Lambda = \kappa/N$, where $\kappa \sim N$ is the effective elasticity of the elastic environment [41].

In Figs. 1(b) and 1(c), we illustrate the typical behavior of the local and global minima of (1) by showing the relation between the applied strain ε and the conjugate stress $\sigma = \Lambda(\varepsilon - X)$, see also [50]. Our Fig. 1(b) shows the brittle behavior, which includes a system size transition from the partially broken to the fully broken state. In contrast, our Fig. 1(c) illustrates the ductile behavior, characterized by the gradual accumulation of damage. The *equilibrium* (global minimum) deformation paths are shown in Fig. 1(b) and 1(c) by thick black lines. We assume that failure is reversible, and show by thin black lines the *out-of-equilibrium* (marginally stable) paths that are different for loading and unloading.

The boundary separating brittle and ductile regimes depends on the strength of the disorder (our parameter ρ) and on the dimensionless parameter

$$\nu = \frac{\lambda}{\Lambda(1+\lambda)}, \quad (2)$$

which we interpret as a measure of the structural *rigidity* of the system [43,51–53]. When ν is small, meaning that either Λ is large or λ is small, individual breakable elements interact weakly and the limit $\lambda \to 0$ can be associated with the (jamming) threshold beyond which the rigidity is lost [11]. Instead, when $\nu \to \infty$ the system can be viewed as overconstrained [9,10].

The ensemble averaged brittleness or ductility threshold can be found by solving the system of equations $-2f(x_c) = f'(x_c)x_c$ and $1 - F(x_c) = f(x_c)x_c - 1/\nu$, where $F(x) = \int_0^x f(x')dx'$ is the cumulative distribution of thresholds [50]. In particular, for Weibull-distributed thresholds, the line separating brittle from ductile behavior is given by the $\nu = \nu_* = \exp(1/\rho + 1)/\rho$, see Fig. 2(a).

In the limit $N \to \infty$ the avalanche distribution in the model (1) can be computed analytically [36,50]

$$p(s) = \frac{s^{s-1}}{s!}\int_0^{\infty}\frac{[1 - g(x)]f(x)}{g(x)}e^{-h(x)s}dx, \quad (3)$$

where $g(x) = f(x)x/[1 - F(x) + \nu^{-1}]$, and $h(x) = g(x) - \ln g(x)$. In the large-event-size asymptotics the universal preintegral multiplier $s^{s-1}/s! \sim s^{-3/2}$ represents the classical mean-field contribution, reflecting the built-in statistics of Brownian return times [39,54]. In the limit $s \to \infty$ the integrated distribution can be obtained by the saddle point approximation around the global minimum, x_0, of the function $h(x)$ [55]. It is a root of either $g(x_0) = 1$ or $g'(x_0) = 0$, and the emergence of such two cases is a general feature of mean-field models [56].

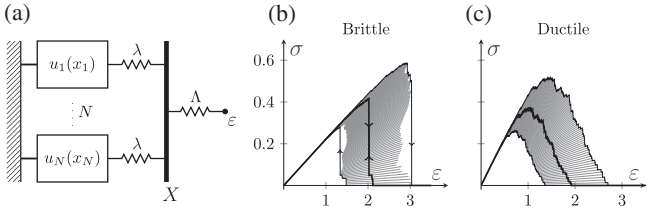

FIG. 1. (a) Schematic representation of the system; (b) brittle response at $\Lambda = 0.4$; (c) ductile response at $\Lambda = 5$. Solid black lines: equilibrium path, thin black line: out-of-equilibrium paths; grey lines: metastable states. Parameters: $N = 100$, $\lambda = 1$, $\rho = 4$.

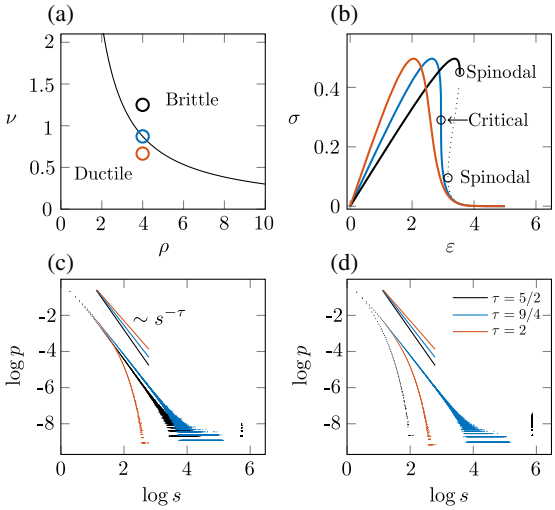

FIG. 2. (a) Ensemble averaged brittle-to-ductile transition line; (b) typical averaged stress-strain curves; (c) nonequilibrium avalanche distribution; (d) equilibrium avalanche distribution. Parameters: $N = 10^6$, $\lambda = 1$. The avalanche distributions was averaged over 10^4 realizations.

Consider first the out-of-equilibrium path (dynamic avalanches). Then, if $g'(x_0) = 0$ while $g(x_0) \neq 1$, we obtain $p(s) \sim s^{-2} e^{-s[h(x_0)-1]}$. This is a subcritical distribution describing the ductile (POP) regime [57], dominated by uncorrelated random events. If $g(x_0) = 1$ but $g'(x_0) \neq 0$, the point x_0 is spinodal, and the distribution is supercritical, characterizing the brittle (SNAP) regime [57]. Neglecting the system-size events, we can write the corresponding local distribution in the form $p(s,x) \sim s^{-3/2}(x-x_0) e^{-s\frac{g'(x_0)^2}{2}(x-x_0)^2}$. The avalanche size diverges near x_0, and the integrated distribution takes the classical form $p(s) \sim s^{-5/2}$ [36]. Finally, if $g(x_0) = 1$ and $g'(x_0) = 0$, the local distribution reads $p(s,x) \sim s^{-3/2}(x-x_0)^2 e^{-s\frac{g''(x_0)^2}{4!}(x-x_0)^4}$. The characteristic avalanche size again diverges near x_0 and the integrated distribution takes the form $p(s) \sim s^{-9/4}$. This is the critical (crackling) regime [57] associated with brittle-to-ductile transition; the exponent $9/4$ has appeared previously in the context of composite FBM involving breakable and unbreakable springs [59]. Other values of the exponents also appeared in the more complex FBM based models describing richer physics [60].

The computed critical exponents coincide with the ones known for the mean-field RFIM [14,61], because the energy (1) can be mapped on the soft-spin RFIM. To this end we need to minimize out the variable X, which gives $\mathcal{H} = -(1/N^2)\sum_{i,j} J x_i x_j - (1/N)\sum_i [H x_i - v_i(x_i)]$, where $v_i(x) = u_i(x) + x^2 + \lambda\Lambda\varepsilon/2(\lambda+\Lambda)$, see also [50]. Note that the Lennard-Jones type potential $u_i(x)$ was transformed along the way into the *double-well* potential $v_i(x)$. Other mean-field formulations leading to the same spinodal and critical exponents that are relevant for amorphous plasticity are discussed in [18,24]; the same two main regimes have been also identified for some sandpile automata [56]. Interestingly, a numerical analysis of a *nonmean-field* model of a structural phase transition reveals the possibility of a similar coexistence of two scaling behaviors [4].

In finite size systems, the crossover from the *robust* spinodal scaling in the brittle regime (exponent $5/2$) to the *nonrobust* critical scaling (exponent $9/4$) takes place in an extended transition zone, where the system exhibits nonuniversal exponents, see Fig. 3. The ubiquity of such "transitional" phenomena may explain the large scatter in reported scaling behavior of disordered solids [62–64].

The mean-field model (1) can be used to demonstrate directly the *superuniversality* of the critical regime [42,66–69]. For instance, one can show that the exponent $9/4$ is valid for both out-of-equilibrium and equilibrium paths [50]. Instead, the spinodal criticality, which exists in the out-of-equilibrium model, disappears in the equilibrium model because the SNAP event takes place before the spinodal point is reached. Integrating the avalanches should be then performed only up to some Maxwellian $x_* < x_0$,

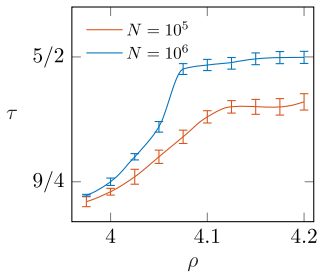

FIG. 3. Finite size crossover associated with brittle to ductile transition. Each curve gives the value of the scaling exponent averaged over 250 realizations. Parameters $\lambda = 1$ and $\nu = 0.873$ (critical value at $\rho = 4$). The exponents and the uncertainty were computed using the maximum likelihood method [65].

and since in this case the function $h(x)$ attains its minimum at the boundary, we obtain $p(s) \propto s^{-5/2} e^{-s[1-h(x_*)]}$. While this distribution has the same exponent $5/2$ as in the case of the out-of-equilibrium path, the scaling is now obscured by the exponential cut off.

We now turn to an intriguing analogy between the equilibrium version of the model (1) and Burgers turbulence [47]. If we minimize out the variables x_i in (1) and consider the thermodynamic limit $N \to \infty$ [50], the equilibrium problem reduces to finding $\tilde{\mathcal{H}}(\epsilon,\nu) \sim \min_{X\in\mathbb{R}}\{\frac{1}{2\nu}(\epsilon - X)^2 + q^\infty(X)\}$, where $q^\infty(z) = [1 - F(\sqrt{\lambda/(\lambda+1)}z)](z^2/2) + \sqrt{\lambda/(\lambda+1)}\int_0^z f(\sqrt{\lambda/(\lambda+1)}z')(z'^2/2)dz'$. We can now use the Hopf-Lax formula [70] to turn this variational problem into a Cauchy problem for a Hamilton-Jacobi equation $\partial_\nu \tilde{\mathcal{H}} + \frac{1}{2}(\partial_\epsilon \tilde{\mathcal{H}})^2 = 0$, where the rigidity ν plays the role of time. This equation must be supplemented by the initial condition $\tilde{\mathcal{H}}(\varepsilon,0) = q^\infty(\varepsilon)$. Then the tension $\sigma = \partial_\epsilon \tilde{\mathcal{H}}$ satisfies the inviscid Burgers equation

$$\partial_\nu \sigma + \sigma \partial_\epsilon \sigma = 0, \tag{4}$$

with the initial condition $\sigma_0 = \partial_\epsilon q^\infty(\varepsilon)$. Interestingly, the viscous Burgers equation for σ and the corresponding KPZ equation [71] for $\tilde{\mathcal{H}}$ emerge as a finite size effect in the model (1) with finite temperature.

As a result of the reduction of the problem (1) to (4), avalanches become shock waves [45]. In the averaged model, the ductile-to-brittle transition can be then associated with the shock formation at a finite value of rigidity $\nu_* = \min_{\varepsilon\in\mathbb{R}}\{-1/\partial_\varepsilon \sigma_0(\varepsilon)\}$, see Fig. 4(b); in the (ε,ν) plane this "event" becomes a direct analog of the liquid-vapor critical point.

At finite N, the "evolution" equation for the stress remains the same as in the case $N \to \infty$, while the initial condition changes to $\sigma_0 = \partial_\varepsilon q(\varepsilon) = N^{-1}\sum_{i=i}^N \varepsilon\Theta(l_i - \sqrt{[\lambda/(\lambda+1)]}\varepsilon)$, see [50] for details. In Fig. 4(a) we show how the increase of rigidity transforms the ductile response, where avalanches take the form of small Burgers shocks (POP events), into the brittle response with a single Burgers

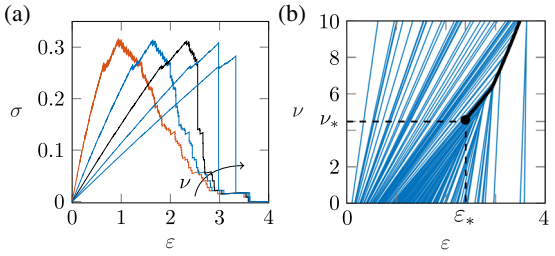

FIG. 4. (a) Time (rigidity) evolution of the randomly distributed initial Burgers data $\sigma_0(\varepsilon)$ (red) at $\rho = 2$, and $\lambda = 1$; black line corresponds to $\nu_* = \exp(1/\rho + 1)/\rho$. (b) Shock merging with critical complexity appearing at $\nu = \nu_*$. Thick black line shows the shock in the averaged system which emerges in the limit $N \to \infty$.

shock representing a system size SNAP event. In Fig. 4(b) we track the position of individual shocks and visualize their merging sequence.

To highlight the *critical* nature of the system with rigidity value close to ν_*, we studied the ν dependence of the number of shocks n. In Fig. 5, we show the standard deviation $\Delta n = [K^{-1}\sum_{i=1}^{K}(n_i - K^{-1}\sum_{i=1}^{K} n_i)^2]^{1/2}$, where different realizations of disorder are indexed by $i = 1, 2, \ldots, K$. Note the peak indicating the anomalous broadening of the distribution around the critical point $\nu = \nu_*$. The situation is fundamentally different in the conventional decaying Burgers turbulence where the initial data have *zero* average, which infinitely delays the emergence of scaling.

So far we were assuming that the rigidity measure ν is finite as $N \to \infty$. A broader class of elastic environments can be modeled if we assume that $\kappa \sim N^{\alpha}$, with $0 \le \alpha \le 1$. For instance, if the load is transmitted through a surface of a 3D body we have $\alpha = 2/3$ and $\nu \sim N^{1/3}$. In this setting, small systems would be necessarily ductile, while brittle behavior would dominate in the thermodynamic limit. At a given disorder, the scaling will be then seen in a window of system sizes, while the (percolation type) critical regime will emerge only at infinite size and infinite disorder [6,7,72].

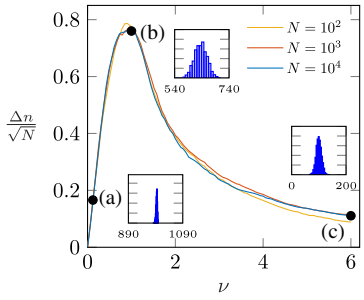

FIG. 5. Time (rigidity) evolution of the normalized standard deviation for the number of shocks. The statistics was obtained from $K = 1000$ realizations of the quenched disorder with $\rho = 3$, and $\lambda = 1$. Inset plots: (a) $\nu = 0.1$ (b) $\nu = 1$; (c) $\nu = 6$.

To conclude, we used an analytically transparent model to quantify the role of system's rigidity (global connectivity) as a control parameter for the transition from brittle to ductile failure. We showed that this transition can be associated with the crossover from spinodal to classical criticality, generating, in finite size systems, a scaling region with nonuniversal exponents. Such behavior is generic for a broad class of systems, encompassing fracture, plasticity, structural phase transitions, and now we established a new link to fluid turbulence.

The authors are grateful to R. Garcia-Garcia, K. Dahmen, and M. Mungan for helpful discussions. H. B. R. was supported by a PhD fellowship from Ecole Polytechnique; L. T. was supported by Grant No. ANR-10-IDEX-0001-02 PSL.

*hudson.borja-da-rocha@college-de-france.fr
†lev.truskinovsky@espci.fr

[1] H. Herrmann and S. Roux, *Statistical Models for the Fracture of Disordered Media*, Random Materials and Processes (Elsevier Science, North Holland, 2014).
[2] M. J. Alava, P. K. V. V. Nukala, and S. Zapperi, Adv. Phys. **55**, 349 (2006).
[3] I. Procaccia, C. Rainone, and M. Singh, Phys. Rev. E **96**, 032907 (2017).
[4] F.-J. Pérez-Reche, L. Truskinovsky, and G. Zanzotto, Phys. Rev. Lett. **101**, 230601 (2008).
[5] D. S. Fisher, K. Dahmen, S. Ramanathan, and Y. Ben-Zion, Phys. Rev. Lett. **78**, 4885 (1997).
[6] R. Toussaint and A. Hansen, Phys. Rev. E **73**, 046103 (2006).
[7] A. Shekhawat, S. Zapperi, and J. P. Sethna, Phys. Rev. Lett. **110**, 185505 (2013).
[8] S. Roy, S. Biswas, and P. Ray, Phys. Rev. E **96**, 063003 (2017).
[9] M. M. Driscoll, B. G.-g. Chen, T. H. Beuman, S. Ulrich, S. R. Nagel, and V. Vitelli, Proc. Natl. Acad. Sci. U.S.A. **113**, 10813 (2016).
[10] L. Zhang, D. Z. Rocklin, L. M. Sander, and X. Mao, Phys. Rev. Mater. **1**, 052602 (2017).
[11] C. P. Goodrich, A. J. Liu, and S. R. Nagel, Nat. Phys. **10**, 578 (2014).
[12] R. L. B. Selinger, Z.-G. Wang, W. M. Gelbart, and A. Ben-Shaul, Phys. Rev. A **43**, 4396 (1991).
[13] J. B. Rundle and W. Klein, Phys. Rev. Lett. **63**, 171 (1989).
[14] S. Zapperi, P. Ray, H. E. Stanley, and A. Vespignani, Phys. Rev. Lett. **78**, 1408 (1997).
[15] A. Wisitsorasak and P. G. Wolynes, Proc. Natl. Acad. Sci. U.S.A. **109**, 16068 (2012).
[16] Y. Moreno, J. B. Gómez, and A. F. Pacheco, Phys. Rev. Lett. **85**, 2865 (2000).
[17] J. V. Andersen, D. Sornette, and K.-t. Leung, Phys. Rev. Lett. **78**, 2140 (1997).
[18] M. Ozawa, L. Berthier, G. Biroli, A. Rosso, and G. Tarjus, Proc. Natl. Acad. Sci. U.S.A. **115**, 6656 (2018).
[19] M. Sahimi and S. Arbabi, Phys. Rev. Lett. **68**, 608 (1992).

[20] S. Roux, A. Hansen, H. Herrmann, and E. Guyon, J. Stat. Phys. **52**, 237 (1988).
[21] A. Hansen and J. Schmittbuhl, Phys. Rev. Lett. **90**, 045504 (2003).
[22] R. Toussaint and S. R. Pride, Phys. Rev. E **71**, 046127 (2005).
[23] A. A. Moreira, C. L. N. Oliveira, A. Hansen, N. A. M. Araújo, H. J. Herrmann, and J. S. Andrade, Phys. Rev. Lett. **109**, 255701 (2012).
[24] M. Popović, T. W. J. de Geus, and M. Wyart, Phys. Rev. E **98**, 040901 (2018).
[25] B. Kahng, G. G. Batrouni, S. Redner, L. de Arcangelis, and H. J. Herrmann, Phys. Rev. B **37**, 7625 (1988).
[26] F. Yuan and L. Huang, Sci. Rep. **4**, 5035 (2014).
[27] J. Liu, Z. Zhao, W. Wang, J. W. Mays, and S.-Q. Wang, J. Polym. Sci. B **57**, 758 (2019).
[28] D. Şopu, A. Foroughi, M. Stoica, and J. Eckert, Nano Lett. **16**, 4467 (2016).
[29] G. Subhash, Q. Liu, and X.-L. Gao, Int. J. Impact Eng. **32**, 1113 (2006).
[30] J. Zhao, X.-T. Feng, X.-W. Zhang, Y. Zhang, Y.-Y. Zhou, and C.-X. Yang, Eng. Geol. **232**, 160 (2018).
[31] M. Selezneva, Y. Swolfs, A. Katalagarianakis, T. Ichikawa, N. Hirano, I. Taketa, T. Karaki, I. Verpoest, and L. Gorbatikh, Composites A **109**, 20 (2018).
[32] D. Krajcinovic, S. Mastilovic, and M. Vujosevic, Meccanica **33**, 363 (1998).
[33] R. Christensen, Z. Li, and H. Gao, Proc. R. Soc. A **474**, 20180361 (2018).
[34] S. Papanikolaou, J. Thibault, C. Woodward, P. Shanthraj, and F. Roters, arXiv:1707.04332.
[35] E. Berthier, J. E. Kollmer, S. E. Henkes, K. Liu, J. M. Schwarz, and K. E. Daniels, arXiv:1812.07466.
[36] A. Hansen, P. Hemmer, and S. Pradhan, *The Fiber Bundle Model: Modeling Failure in Materials*, Statistical Physics of Fracture and Breakdown (Wiley-VCH, 2015).
[37] F. T. Peirce, J. Textile Ind. **17**, 355 (1926).
[38] H. Nechad, A. Helmstetter, R. E. Guerjouma, and D. Sornette, J. Mech. Phys. Solids **53**, 1099 (2005).
[39] D. Sornette, J. Phys. I (France) **2**, 2089 (1992).
[40] P. C. Hemmer and A. Hansen, J. Appl. Mech. **59**, 909 (1992).
[41] A. Delaplace, S. Roux, and G. P. jaudier Cabot, Int. J. Solids Struct. **36**, 1403 (1999).
[42] I. Balog, M. Tissier, and G. Tarjus, Phys. Rev. B **89**, 104201 (2014).
[43] M. Merkel, K. Baumgarten, B. P. Tighe, and M. L. Manning, Proc. Natl. Acad. Sci. U.S.A. **116**, 6560 (2019).
[44] J. R. Rice, Fract. Mech. Ceram. **2**, 191 (1968).
[45] J.-P. Bouchaud and M. Mézard, J. Phys. A **30**, 7997 (1997).
[46] P. Le Doussal and K. J. Wiese, Phys. Rev. E **79**, 051106 (2009).
[47] J. Bec and K. Khanin, Phys. Rep. **447**, 1 (2007).
[48] A. Basu and B. K. Chakrabarti, Phil. Trans. R. Soc. A **377**, 20170387 (2019).
[49] If the breakable elements are composed of subparts linked in series and if the failure is associated with breaking of the weakest subpart, the Weibull distribution emerges rigorously in the thermodynamic limit as the distribution for the breaking threshold of the whole system. Here we assume that the distribution of thresholds for the subparts has a compact support.
[50] See Supplemental Material at http://link.aps.org/supplemental/10.1103/PhysRevLett.124.015501 for the study of the structure of the metastable states, the computation of the statistics of avalanche distribution, mapping on the RFIM and the reduction to Burgers model in the case of finite N.
[51] M. F. J. Vermeulen, A. Bose, C. Storm, and W. G. Ellenbroek, Phys. Rev. E **96**, 053003 (2017).
[52] H. Crapo, Struct. Topol. **1979**, 1 (1979).
[53] J. Z. Kim, Z. Lu, S. H. Strogatz, and D. S. Bassett, Nat. Phys. **15**, 714 (2019).
[54] S. Zapperi, K. B. Lauritsen, and H. E. Stanley, Phys. Rev. Lett. **75**, 4071 (1995).
[55] Our asymptotic analysis is valid for arbitrary disorder as long as the function $h(x)$ has a minimum. Some long tailed disorders can modify the behavior of the system, for instance, the distribution of thresholds $F(x) = 0$, for $x \leq 1$, and $F(x) = 1 - 1/\sqrt{x}$, for $x > 1$, leads to the function $h(x)$ without a minimum.
[56] S. di Santo, R. Burioni, A. Vezzani, and M. A. Muñoz, Phys. Rev. Lett. **116**, 240601 (2016).
[57] Here SNAP corresponds to supercritical regimes which include isolated system size avalanches, POP describes subcritical regimes with uncorrelated events distributed around an average size, and the terms "CRAKLE" and "crackiling" are used for critical regimes with scale-free avalanches [4,58].
[58] J. P. Sethna, K. A. Dahmen, and C. R. Myers, Nature (London) **410**, 242 (2001).
[59] R. C. Hidalgo, K. Kovács, I. Pagonabarraga, and F. Kun, Europhys. Lett. **81**, 54005 (2008).
[60] R. C. Hidalgo, F. Kun, K. Kovács, and I. Pagonabarraga, Phys. Rev. E **80**, 051108 (2009).
[61] K. Dahmen and J. P. Sethna, Phys. Rev. B **53**, 14872 (1996).
[62] J. Weiss, W. B. Rhouma, T. Richeton, S. Dechanel, F. Louchet, and L. Truskinovsky, Phys. Rev. Lett. **114**, 105504 (2015).
[63] Y. Xu, A. G. Borrego, A. Planes, X. Ding, and E. Vives, Phys. Rev. E **99**, 033001 (2019).
[64] G. Sparks and R. Maaß, Phys. Rev. Mater. **2**, 120601 (2018).
[65] A. Clauset, C. R. Shalizi, and M. E. J. Newman, SIAM Rev. **51**, 661 (2009).
[66] F. J. Pérez-Reche and E. Vives, Phys. Rev. B **70**, 214422 (2004).
[67] A. Maritan, M. Cieplak, M. R. Swift, and J. R. Banavar, Phys. Rev. Lett. **72**, 946 (1994).
[68] Y. Liu and K. A. Dahmen, Phys. Rev. E **79**, 061124 (2009).
[69] I. Balog, G. Tarjus, and M. Tissier, Phys. Rev. B **97**, 094204 (2018).
[70] L. C. Evans, *Partial Differential Equations*, Graduate Studies in Mathematics, Vol. 19 (American Mathematical Society, Providence, 2010).
[71] M. Kardar, G. Parisi, and Y.-C. Zhang, Phys. Rev. Lett. **56**, 889 (1986).
[72] Z. Olami, H. J. S. Feder, and K. Christensen, Phys. Rev. Lett. **68**, 1244 (1992).